

# Physicochemical properties and desulfurization activities of metal oxide/biomass-based activated carbons prepared by blending method

Lu Fan · Xia Jiang · Wenju Jiang · Jiaxiu Guo · Jie Chen

Received: 1 December 2013 / Revised: 11 May 2014 / Accepted: 16 June 2014 / Published online: 25 June 2014  
© Springer Science+Business Media New York 2014

**Abstract** Column activated carbons were prepared from walnut shell chars and transition metal oxide powders (i.e.  $\text{Co}_2\text{O}_3$ ,  $\text{Ni}_2\text{O}_3$ ,  $\text{CuO}$  and  $\text{V}_2\text{O}_5$ ) with blending method. Samples were characterized by  $\text{N}_2$  adsorption–desorption, X-ray diffraction, X-ray photoelectron spectroscopy and Fourier-transform infrared spectroscopy. The texture properties of all modified activated carbons with metal oxides dosage of  $<5$  wt% did not change evidently. The basic functionalities of these activated carbons increased relative to blank carbon. Moreover, metal species with different oxidation states coexisted on the modified activated carbons. The optimal dosage of all metal oxides was 2 wt%. The sulfur capacities of these modified activated carbons were 7.7–46.0 % higher than that of blank activated carbon and the highest occurred for  $\text{V}_2\text{O}_5$  modified activated carbon. The improved desulfurization performance was mainly attributed to the higher catalytic activity of the active metal oxides formed in the presence of  $\text{O}_2$  during the desulfurization process.

**Keywords** Walnut shell · Activated carbon · Transition metals · Blending method · Desulfurization activity

## 1 Introduction

Activated carbon is a carbonaceous adsorbent with high porosity, large surface area, variable surface chemistry characteristics and high surface reactivity. Activated carbon is widely used for environmental pollution control and in industrial processes as both adsorbent and catalyst. Among these applications, activated carbon based dry flue gas desulfurization methods attract worldwide attention due to their distinct advantages, such as their relatively simple procedures and higher  $\text{SO}_2$  removal relative to wet scrubbing (Guo and Lua 2002). However, a large amount of activated carbon must be used in this process because the  $\text{SO}_2$  capacity of normal activated carbon is low and can only be applied at low space velocity. Thus, this application can be very expensive. Therefore, it is important to develop a novel activated carbon from inexpensive raw materials with improved desulfurization activity.

Some agriculture byproducts are both inexpensive and abundantly available. In China, more than 1,00,000 tons of walnut shells are produced yearly (Yang and Qiu 2010). The reutilization of such wastes is useful for waste disposal and for exploiting their economic value. Walnut shells have high carbon content and low ash content, which makes them a good precursor for activated carbon production. Currently, it has been successfully applied for wastewater treatment (for example, the adsorption of dyes, heavy metal ions, etc.) (Kazemipour et al. 2008; Yang and Qiu 2010; Zabihi 2010). Nevertheless, little research has been conducted regarding the use of activated carbon derived from walnut shells for the removal of  $\text{SO}_2$  from flue gas.

In addition, previous studies have found that the desulfurization activities of activated carbon could be improved by modification with transition metals, such as Co, Ni, Cu

L. Fan · X. Jiang · W. Jiang (✉) · J. Guo · J. Chen  
College of Architecture and Environment, Sichuan University,  
Chengdu 610065, People's Republic of China  
e-mail: wenjujiang@scu.edu.cn

W. Jiang · J. Guo  
National Engineering Research Center for Flue Gas  
Desulfurization, Chengdu 610065, China

and V (Gao et al. 2011; Guo et al. 2012; Tseng et al. 2003). Several procedures can be used practically to prepare activated carbon support catalysts. These procedures involve impregnation and blending methods. Impregnation methods generally include the addition of additives on as-received activated carbon, and followed by loaded activated carbon be calcined at 400–800 °C. In contrast, the blending method is performed by blending the carbon chars with additives before activation at 800–900 °C. This method is relatively simple and is referred to as one-step activation. Another difference between these two loading methods is the use of additive forms. Both solids and solutions can be used as additives for modifying activated carbon by blending method, but only solutions can be used when impregnation method is applied. Impregnation method has been widely used and studied (Afrane and Achaw 2008; Fan et al. 2012), however, very few studies regarding blending method have been published (Przepiórski 2005). The metal oxide is only distributed on the surface of activated carbon following impregnation method. In contrast, blending method results in the uniform distribution of additives throughout the carbon matrix (Przepiórski et al. 1999). In this study, the unique characteristics of blending method and the high temperature (900 °C in this study) used for metal oxides/carbon char activation are hypothesized to affect the physicochemical properties of the modified activated carbon, including the texture properties, functional groups and metal speciation. These properties are important factors that govern the sulfur capacity of activated carbon.

Therefore, the objective of this work was to investigate the effects of metal oxide blending on the physicochemical properties and SO<sub>2</sub> removal performance of activated carbon. First, transition metal oxides powders (Co<sub>2</sub>O<sub>3</sub>, Ni<sub>2</sub>O<sub>3</sub>, CuO and V<sub>2</sub>O<sub>5</sub>) were blended with walnut shell carbon chars. Next, the activated carbon was produced with one-step activation. The characterization and desulfurization activities of modified activated carbon were examined. Moreover, the possible desulfurization mechanisms of this novel catalyst were deduced.

## 2 Materials and methods

### 2.1 Preparation of activated carbon

Walnut shells used as the raw material for activated carbon preparation were obtained from Sichuan province, P. R. China. Elemental analysis showed that the walnut shells mainly consisted of (wt %): C 48.99 %, H 5.74 %, O 45.03 %, and N 0.24 %.

The walnut shells were crushed and sieved to obtain a final particle size of 0.14–0.28 mm. Next, the particles

were carbonized in an electric furnace (SX2-8-10P, Chengdu, China) at 600 °C for 1 h at a constant heating rate of 5 °C/min. Subsequently, the chars were ground and passed through a 200-mesh screen before mixing with fine metal oxide powders (Co<sub>2</sub>O<sub>3</sub>, Ni<sub>2</sub>O<sub>3</sub>, CuO and V<sub>2</sub>O<sub>5</sub>, respectively) at weight ratios of 2, 5, 7 and 10 %, respectively. Afterwards, the mixtures were combined with hot coal tar (at approximately 60 °C), which served as the major binder, and carboxyl methyl cellulose (CMC) and/or polyvinyl butyral resin (PVB), which served as accessorial binders. These mixtures were stirred thoroughly in a 70 °C water bath before molding in a vacuum extruder a 3 mm diameter column. After formation, the molded carbon columns were activated at a temperature of 900 °C with a CO<sub>2</sub> flow of 1,000 mL/min for 2 h.

The prepared column activated carbons were named AC, AC-Co, AC-Ni, AC-Cu and AC-V based on the metal oxides that were used for modification. A weight percentage attached refers to the metal oxide dosage.

### 2.2 Activated carbon characterization

The BET surface area, pore volume and pore size distribution were calculated by nitrogen adsorption–desorption isotherms, obtained with an AUTOSORP ZXF-6 vacuum volumetric sorption instrument. X-ray diffraction (XRD) patterns were obtained with an X' PertPro MPD diffractometer at 30 kV and 20 mA employing Cu K $\alpha$  radiation and step-scanning over 2 $\theta$  range 10–80°. X-ray photoelectron spectra (XPS) analysis was applied to determine the surface chemical composition and functional groups with an ESCALAB 250XI spectrometer (Thermo Scientific, USA) using Al K $\alpha$  radiation (1486.6 eV). XPS analysis was performed before and after the samples were etched using a 3 kV Ar<sup>+</sup> ion beam for 5 min. For Fourier-transform infrared spectroscopy (FTIR) characterization, a fixed weight of each sample was mixed with KBr before analysis. Transmission measurements were carried out in the 4,000–400 cm<sup>−1</sup> region with a spectrometer (FTIR 670 NEXUS Nicolet, USA) at a resolution of 4 cm<sup>−1</sup>. The content of surfaces site with acidic and basic characteristics were determined by the adsorption of benzoic acid (BA) and diphenylguanidine (DPG), respectively (Davini 1989).

### 2.3 Desulfurization experiment

The desulfurization experiments were carried out in a fixed-bed reactor system. A synthetic flue gas that contained 5,000 mg/m<sup>3</sup> SO<sub>2</sub>, 9 vol% O<sub>2</sub>, 10 vol% water vapor and was balanced by N<sub>2</sub> was preheated to 80 °C and passed through the columnar reactor (18 × 300 mm). This column contained 15 g of activated carbon at a space velocity of 600 h<sup>−1</sup>. The SO<sub>2</sub> concentration was determined by

**Table 1** Texture properties of activated carbons

Activated carbon	BET (m <sup>2</sup> /g)	V total (cm <sup>3</sup> /g)	Average pore radius (nm)
AC	565	0.380	1.565
AC-Co2	515	0.349	1.360
AC-Co5	641	0.420	1.855
AC-Co10	411	0.320	1.560
AC-Ni2	533	0.330	1.611
AC-Ni5	216	0.143	1.320
AC-Ni10	379	0.247	1.310
AC-Cu2	520	0.310	1.702
AC-Cu5	458	0.290	1.270
AC-Cu10	420	0.262	1.250
AC-V2	589	0.360	1.678
AC-V5	373	0.222	1.190
AC-V10	259	0.162	1.250

measuring the H<sub>2</sub>SO<sub>4</sub> concentration with a NaOH solution after passing the gaseous mixture through a H<sub>2</sub>O<sub>2</sub> solution. The amount of SO<sub>2</sub> removed was calculated by integrating the curves of outlet SO<sub>2</sub> concentration with time. Break-through occurred when the outlet SO<sub>2</sub> concentration was 100 ppm.

### 3 Results and discussion

#### 3.1 Physicochemical properties of prepared activated carbons

##### 3.1.1 Texture properties

Table 1 contains the texture properties of the prepared activated carbons, including the BET surface area, total pore volume and average pore radius. When metal oxides were added at 2 wt%, the texture properties of modified activated carbon did not change significantly. The surface area and pore volume for the AC-Co2, AC-Ni2, and AC-Cu2 samples decreased slightly, and the surface area of AC-V2 was more developed relative to AC. At a loading ratio of 2 wt%, the surface area increased in the following order: AC-Co2 < AC-Cu2 < AC-Ni2 < AC-V2. When the loading ratio increased to 5 wt%, the surface area and pore volume of all modified activated carbons decreased considerably, especially for AC-Ni5. However, AC-Co5 had a higher surface area (641 m<sup>2</sup>/g) and total pore volume (0.420 cm<sup>3</sup>/g) than that of AC (565 m<sup>2</sup>/g and 0.380 cm<sup>3</sup>/g).

The dosage of metal oxides significantly affected the development of texture properties of activated carbon. Apparently, the metal oxide dose should not exceed 5 wt% when blending method is used to modify activated carbon.

Using proper loading ratio of metals promotes the formation of specific porosity due to the reaction between the added metal oxides and the carbon substrate during carbon gasification process. However, excess addition of metal particles may promote aggregation and the formation of large crystals during preparation. This process would result in pore blockage and surface area decrease (Nguyen-Thanh and Bandosz 2003; Lee et al. 2002).

#### 3.2 Surface functionalities

XPS analysis was employed to investigate the surface functional groups of prepared samples. The C1s spectra of the activated carbon with and without modification are provided in Fig. 1. The C1s binding energy (BE) values for the modified activated carbon were similar to those of blank activated carbon, which suggested carbon properties did not significantly change after modification. All modified activated carbon had four components with BE value of approximately 284.6, 285.7, 287.6 and 289.4 eV. These BE values were assigned to C–C from graphitic carbon, C–O from phenolic etheric or alcoholic carbon, C=O bonds from carbonyl carbon and COOH bonds from carboxylic or lactonic carbon, respectively. However, difference in the functional groups concentrations of the activated carbons were not pronounced in the XPS spectrums, potentially due to the test limitations of this analytical method. Thus, FTIR was used to determine the development of the surface functional groups after metal addition.

As shown in Fig. 2, the FTIR spectra were similar for all carbon samples, which indicated the presence of similar functional groups on the carbon surface. This result agreed with the result obtained from XPS analysis. Broad peaks at approximated 3,400 cm<sup>−1</sup> were assigned to the O–H stretching vibration of the hydroxyl functional groups (including hydrogen bonding) (Namasivayam and Kavitha 2006). Intensity increments in this position were observed for the Co, Cu and V modified activated carbons, which suggested a possible hydrogen-bonding interaction between the surface hydroxyl groups and the loaded metal oxides (Baltrusaitis et al. 2006). A band occurred at approximately 3,700 cm<sup>−1</sup> in the AC-Co2, AC-Ni2 and AC-V2 samples. This band was due to the presence of hydroxyl groups that were coordinated to one metal atom (Rochester and Topham 1979). However, no peak in this area was detected in the 2 wt% CuO modified carbon sample. The band at 1,630 cm<sup>−1</sup> was likely resulted from the C=O stretching vibration of different functional groups, including quinones and lactones (Sabio et al. 2004). Adsorptions due to C–O vibrations occurred between 1,300 and 900 cm<sup>−1</sup>. The intense band at approximately 1,100 cm<sup>−1</sup> was attributed to the C–O stretching of ether, ester, alcohol and phenol (Cain et al. 2010). The intensity

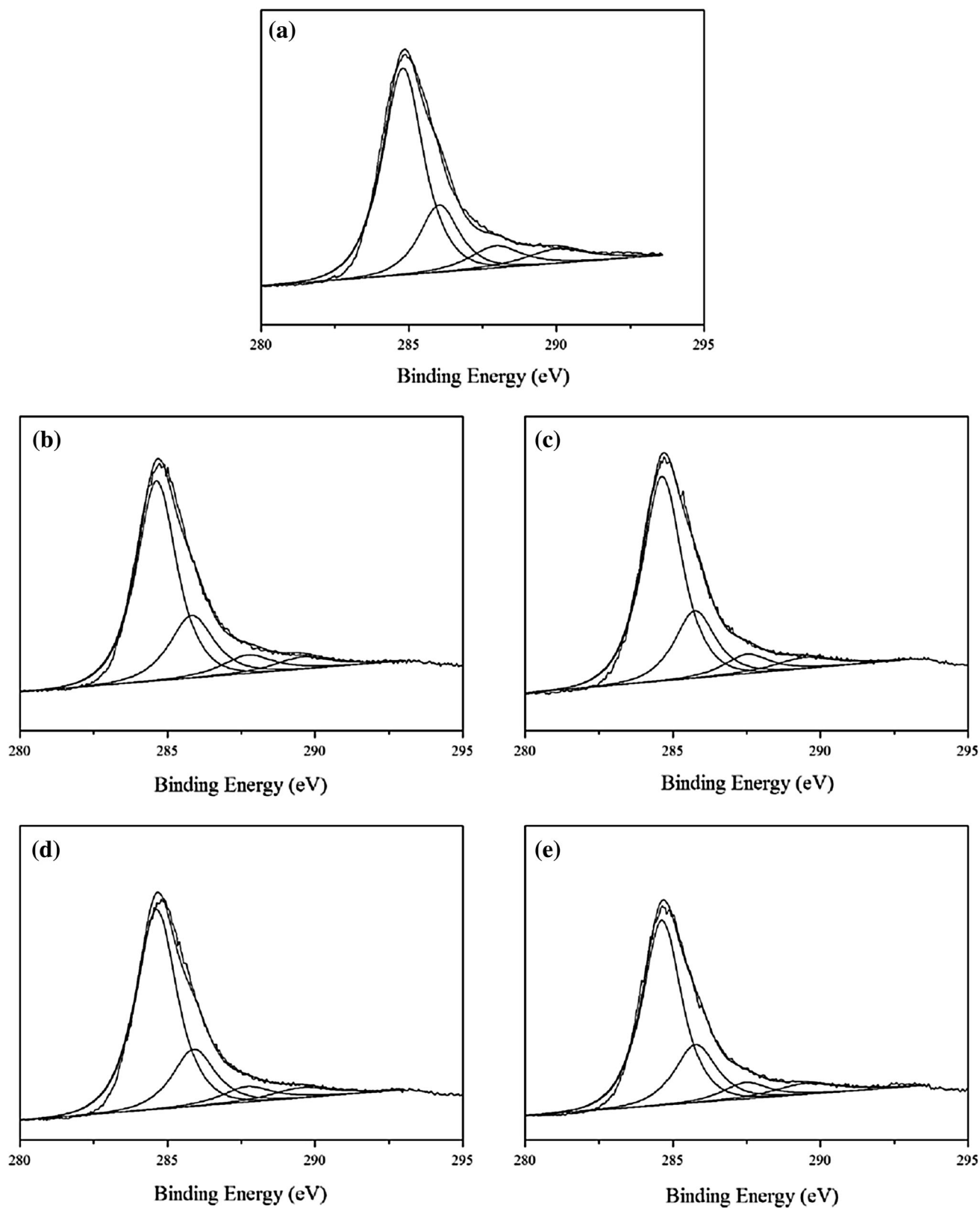


**Fig. 1** The binding energy patterns of C1s for AC (a), AC-Co<sub>2</sub> (b), AC-Ni<sub>2</sub> (c), AC-Cu<sub>2</sub> (d), AC-V<sub>2</sub> (e)





Li et al. 2010). They could have been reduced completely at this high temperature during activation process when the Co species was presented on the surface of the carbon supports. Regarding AC-Ni2, diffraction peaks assigned to Ni were observed at  $2\theta = 44.5^\circ$ ,  $51.8^\circ$  and  $76.4^\circ$ , which (JCPDS 70-1849) (Qin et al. 2008). Except for the presence of metallic nickel, the reduction of  $\text{Ni}_2\text{O}_3$  also caused the formation of NiO, with the reflection at  $37.3^\circ$ ,  $43.3^\circ$  and  $62.9^\circ$  (JCPDS 47-1049) (Wu et al. 2011). For the 2 wt% CuO modified activated carbon, diffraction peaks located at  $43.4^\circ$ ,  $50.05^\circ$  and  $74.1^\circ$  (JCPDS 85-1326) for the presence of Cu and at  $36.7^\circ$ ,  $42.5^\circ$ ,  $61.9^\circ$  and  $73.9^\circ$  (JCPDS 05-0667) for  $\text{Cu}_2\text{O}$  (Kobayashi et al. 2009). This result indicated that Cu and its oxides coexisted on the modified activated carbon. Compared to other samples, more diffraction peaks were observed for AC-V2, including  $\text{V}_2\text{O}_3$  (JCPDS 34-0187),  $\text{V}_2\text{O}_5$  (JCPDS 45-1074) and VO (JCPDS 65-4054). This result occurred because that vanadium species have significant mobility on certain oxide surfaces. And at relatively high concentrations, it is potentially easier for the vanadium species to agglomerate (Gao et al. 2011; Guo et al. 2009).

XPS analysis was conducted for further clarifying the catalytically active species of the metal additives on the modified activated carbons. It is known that the information depth of XPS test is only about 3 nm in general, hence the oxidized metals may cover the activated carbon surface and results in metals with other chemical states unexposed and undetectable by XPS test. For this reason, in this experiment, XPS analysis with the  $\text{Ar}^+$  ion etching procedure was also performed on all metal loaded activated carbons, which was reported to be an effective way to extend the depth of the XPS analysis (Mutel et al. 1995; Paparazzo 1986). The XPS metal spectra of all 2 wt% metal loaded activated carbon samples with and without the  $\text{Ar}^+$  etching procedure are exhibited in Fig. 4. It can be seen from Fig. 4, without etching with  $\text{Ar}^+$  ions, the Co  $2p_{3/2}$  peak around 780.7 eV was observed in sample AC-Co2 due to the presence of  $\text{Co}^{2+}$  (Gautier et al. 1997). For AC-Ni2, the Ni  $2p_{3/2}$  BE was 854.4 eV, which was characteristic of  $\text{Ni}^{2+}$  in NiO (Roh et al. 2001). The strong shake-up line located at 860.8 eV belongs to  $\text{Ni}^{2+}$  species (Wang and Ozkan 2005). For 2 wt% CuO modified activated carbon, the Cu  $2p_{3/2}$  was composed of two components at 933.7 and 942.0 eV, which indicated that the chemical state of copper is  $\text{Cu}^{2+}$  (Sinapi et al. 2002; Guo et al. 2011). The V  $2p_{3/2}$  peak occurred at 517.5 eV, which was assigned to  $\text{V}^{5+}$ . Single peaks at approximately 521.8 eV were reported to result from the reflection of  $\text{V}_2\text{O}$  (Kónya et al. 2004). And with the  $\text{Ar}^+$  etching process (Fig. 4b), peaks at 778.7 and 853.1 eV were detected for sample AC-Co2 and AC-Ni2, which was due to the presence of metallic Co and Ni (Hammond and Winograd 1977; Wang 1998). This is in good agreement with the results

obtained by XRD analysis (Fig. 3). For sample AC-V2, the  $\text{V}2p_{3/2}$  peak was located around 515.4 eV, which was associated with the presence of  $\text{VO}_2$  (Rao et al. 1979). The Cu  $2p_{3/2}$  BE was found around 933.0 eV, which could be attributed to Cu(0) and Cu(I) (Aravinda et al. 2002; Hudak et al. 1990). Same result was also showed in XRD spectra.

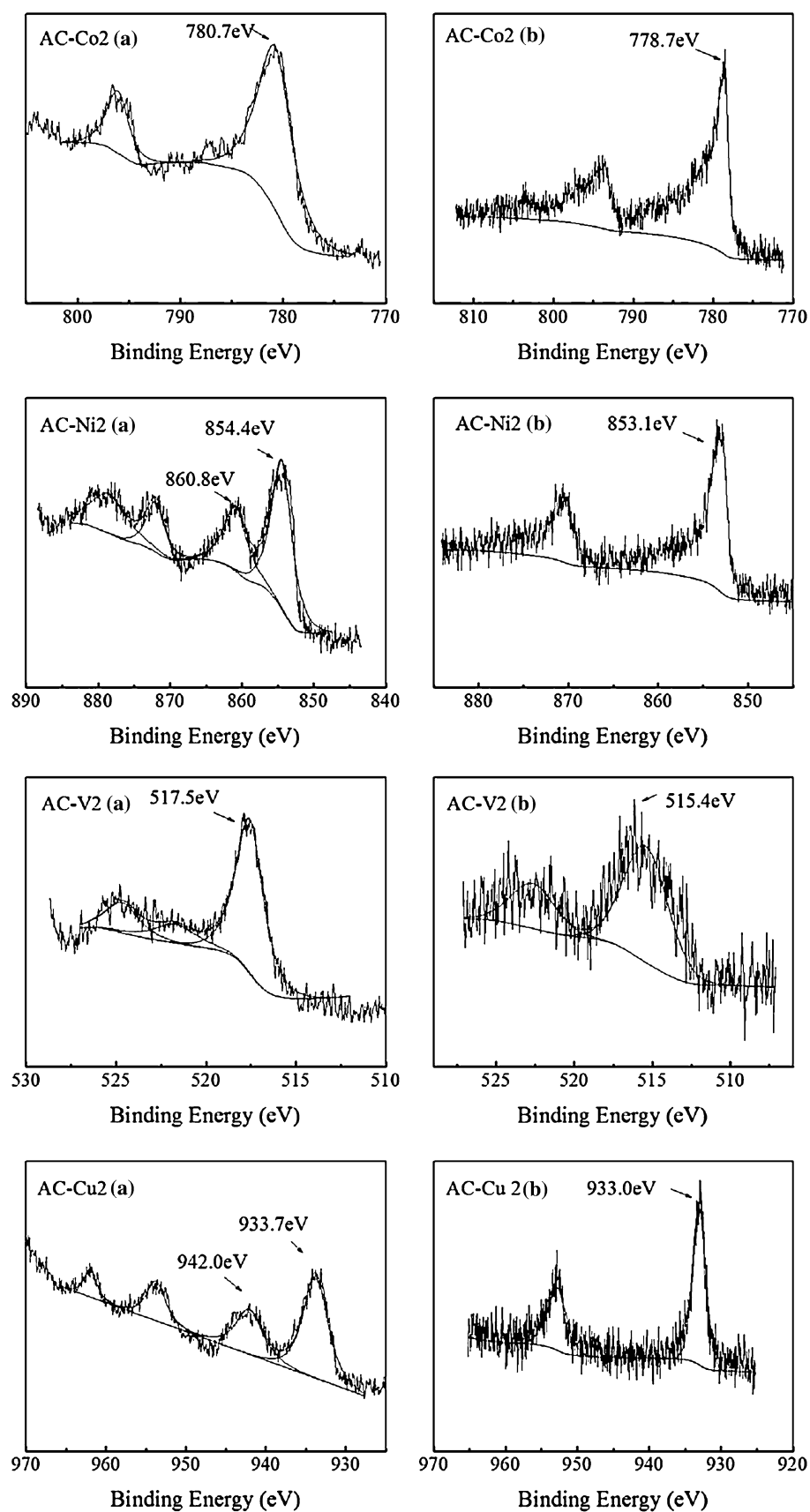
By Combining the XPS and XRD results, reductions in the oxidation state were observed for all modified activated carbon, which occurred because of the blending method that was used in this study (one-step activation process). When heated at 900 °C with carbon materials in a  $\text{CO}_2$  atmosphere these metal oxides were decomposed and then potentially reduced to a lower and more stable oxidation state during their reaction with the carbon substrate. For the AC-Co2, AC-Ni2 and AC-Cu2 samples, some of the additives were completely reduced to their metallic state and coexisted with metal oxides on the carbon surface. Four types of metal species, including  $\text{V}_2\text{O}_5$ ,  $\text{V}_2\text{O}_3$ , VO and  $\text{V}_2\text{O}$  were formed on the carbon surface in the AC-V2 sample. These reduced state and intermediate state metal species are reported to be the primary active species for  $\text{SO}_2$  removal due to their ability to change electron valence (Li et al. 2009).

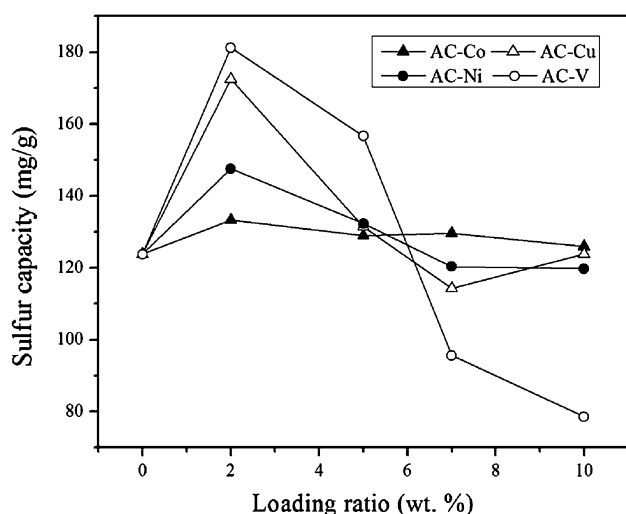
### 3.4 Desulfurization activity tests

Figure 5 presents the  $\text{SO}_2$  breakthrough capacity of activated carbon at different loading ratios (0–10 wt%). The sulfur capacity of blank activated carbon from walnut shells was high (123.8 mg/g), which suggested that walnut shells are good candidate as raw material for producing activated carbon. For carbon samples that were modified with CuO,  $\text{Ni}_2\text{O}_3$  and  $\text{V}_2\text{O}_5$ , respectively, the sulfur capacity increased as the loading ratio increased from 0 to 2 wt% and decreased as the loading ratio increased above 2 wt%. This phenomenon was more evident for the  $\text{V}_2\text{O}_5$  modified activated carbon. Compared with sample AC-V2, the sulfur capacity decreased by 56.6 % when the  $\text{V}_2\text{O}_5$  ratio increased to 10 wt%. However, the desulfurization performance of AC-Co did not significantly change with different doses.

Furthermore, the best desulfurization performance for all modified activated carbon occurred at a loading ratio of 2 wt% for all modified activated carbon (Fig. 5). The sulfur capacities of AC-Co2, AC-Ni2, AC-Cu2 and AC-V2 were 133.3, 147.5, 172.4 and 181.2 mg/g, which were 7.7, 19.1, 39.3 and 46.4 % higher than the AC sulfur capacity, respectively. Vanadium appeared to be the one which most favors  $\text{SO}_2$  sorption onto the carbon matrix. It has been reported that the catalytic activity of V is higher than that of the other metal oxides, such as Co, Ni and Cu (Gao et al. 2011).

**Fig. 4** Metal spectra for the different metal modified activated carbons **a** without and **b** with the  $\text{Ar}^+$  etching procedure





**Fig. 5** Breakthrough sulfur capacities of all samples (with the loading ratio of 0, 2, 5, 7, 10 wt%)

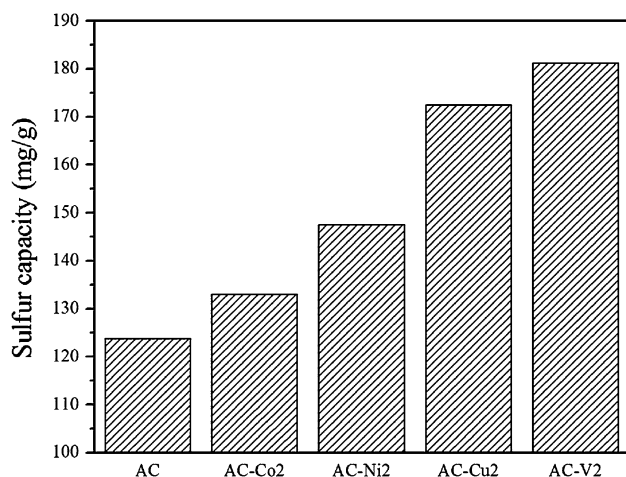
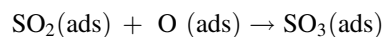
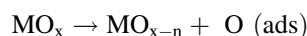
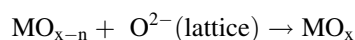


**Fig. 6** Breakthrough sulfur capacity of 2 wt% metal modified activated carbon

Several factors can affect the removal performance of activated carbon for  $\text{SO}_2$ , including the specific surface area, pore-size distribution, pore volume, surface charge, presence of surface functional groups and catalytic activity of the metal species on the carbon surface. As shown in Table 1, the surface area and pore volume decreased considerably the loading ratio of the activated carbon exceeded 5 wt%. This result partially explained the significantly lower sulfur capacities of modified activated carbon with greater metal ratios because higher surface area and total pore volume positively affect  $\text{SO}_2$  removal by carbon materials. For the 2 wt% metal modified activated carbons, the change of surface area and pore volume was not evident. Thus, the development of texture properties was not the main reason for their better desulfurization

performance. It is also noticed that metal addition to activated carbon improved the generation of oxygenate functional groups on the carbon surface (Table 2). The increment of basic functional groups is beneficial for the  $\text{SO}_2$  adsorption process on activated carbon due to the binding affinity. For example, AC-Cu2 possessed the highest basic functional group content and thus exhibited good desulfurization activity (Fig. 6).

Furthermore, the catalytic activities of the metal species resulted in improved desulfurization performance in the modified activated carbon. The oxidation state of the added metal oxides was partly reduced during carbon activation (Figs. 3, 4). In the oxidation catalytic reaction, the gaseous oxygen is first absorbed onto these reduced and intermediate state metal species and converted into the lattice oxygen. Active metal oxides with much higher catalytic activity were then formed by the reaction between the reduced and intermediate state metal species and the lattice oxygen atoms (Doornkamp and Ponc 2000). For example, for AC-V2,  $\text{V}^{3+}$ ,  $\text{V}^{2+}$  and  $\text{V}^{1+}$  species coexisted on the carbon matrix after activation. These vanadium species would be oxidized by  $\text{O}_2$  to active  $\text{V}_2\text{O}_5$ , which possesses a much higher catalytic activity for  $\text{SO}_2$  than  $\text{V}_2\text{O}_5$  (Li et al. 2009). Similar reactions occurred to form active metal oxides in the AC-Co2, AC-Ni2 and AC-Cu2 sample. Next, these active metal oxides reacted with  $\text{SO}_2$  in the desulfurization system to form  $\text{SO}_3$ . Specific mechanism can be described as follows:



This process was followed by  $\text{H}_2\text{SO}_4$  generation with  $\text{H}_2\text{O}$ . The resulting metal species in their low oxidation state would be oxidized by  $\text{O}_2$  in the desulfurization system to form active metal oxides again. It can be seen that this catalytic cycle depends on the change between chemical valences of the metal species. The complex metal species component in AC-V2 could partially explain its higher sulfur capacity compare to the other metal modified activated carbons.

The desulfurization capacity changed greatly when different transition metal oxides were used for activated carbon modification with blending method (Fig. 5). This is related with the variable nature and reaction mechanism of these metals themselves. When an additive dosage of 2 wt% was used, the AC-V2 and AC-Cu2 samples presented a higher  $\text{SO}_2$  removal activity. This finding suggested that these expensive additives could be replaced with less expensive mineral ores or industrial solid wastes



that contain vanadium/copper to produce novel and inexpensive catalysts with high a desulfurization activity.

#### 4 Conclusions

Walnut shell activated carbon was modified with transition metals ( $\text{Co}_2\text{O}_3$ ,  $\text{Ni}_2\text{O}_3$ ,  $\text{CuO}$  and  $\text{V}_2\text{O}_5$ ) by blending method. At the optimal dosage of 2 wt%, the sulfur capacities of the Co, Ni, Cu and V loaded samples and the blank activated carbon were 133.3, 147.5, 172.4, 181.2 and 128.3 mg/g, respectively. The improvement of sulfur capacity mainly resulted from the additional basic functional groups that were generated after modification and the high catalytic activities of the active metal oxides that were formed during the desulfurization process.

**Acknowledgments** This project is financially supported by the National Natural Science Foundation of China (Project No. 51078245).

#### References

- Afrane, G., Achaw, O.W.: Effect of the concentration of inherent mineral elements on the adsorption capacity of coconut shell-based activated carbons. *Bioresour. Technol.* **99**, 6678–6682 (2008)
- Aravinda, C.L., Mayanna, S.M., Bera, P., Jayaram, V., Sharma, A.K.: XPS and XAES investigations of electrochemically deposited Cu-Ni solar selected black coatings on molybdenum substrate. *J. Mater. Sci. Lett.* **21**, 205–208 (2002)
- Baltrusaitis, J., Jensen, J.H., Grassian, V.H.: FTIR spectroscopy combined with isotope labeling and quantum chemical calculations to investigate adsorbed bicarbonate formation following reaction of carbon dioxide with surface hydroxyl groups on  $\text{Fe}_2\text{O}_3$  and  $\text{Al}_2\text{O}_3$ . *J. Phys. Chem. B* **110**, 12005–12016 (2006)
- Balwant, R.P., Bansal, R.C.: Studies in surface chemistry of carbon blacks, part I. High temperature evacuations. *Carbon* **1**, 451–455 (1964)
- Cain, J.P., Gassman, P.L., Wang, H., Laskin, A.: Micro-FTIR study of soot chemical composition—evidence of aliphatic hydrocarbons on nascent soot surfaces. *Phys. Chem. Chem. Phys.* **12**, 5206–5218 (2010)
- Chu, X.W., Liu, J., Sun, B., Dai, R., Pei, Y., Qiao, M.H., Fan, K.N.: Aqueous-phase reforming of ethylene glycol on Co/ZnO catalysts prepared by the coprecipitation method. *J. Mol. Catal. A* **225**, 129–135 (2011)
- Davini, P.: Adsorption of sulphur dioxide on thermally treated active carbon. *Fuel* **68**, 145–148 (1989)
- Davini, P.: Influence of surface properties and iron addition on the  $\text{SO}_2$  adsorption capacity of activated carbons. *Carbon* **40**, 729–734 (2002)
- Doornkamp, C., Ponec, V.: The universal character of the Mars and Van Krevelen mechanism. *J. Mol. Catal. A* **162**, 19–32 (2000)
- Fan, M.M., Zhang, P.B., Ma, Q.K.: Enhancement of biodiesel synthesis from soybean oil by potassium fluoride modification of a calcium magnesium oxides catalyst. *Bioresour. Technol.* **104**, 447–450 (2012)
- Gao, X., Liu, S.J., Zhang, Y., Luo, Z.Y., Cen, K.F.: Physicochemical properties of metal-doped activated carbons and relationship with their performance in the removal of  $\text{SO}_2$  and NO. *J. Hazard. Mater.* **188**, 58–66 (2011)
- Gautier, J.L., Rios, E., Gracia, M., Marco, J.F., Gancedo, R.: Characterization by X-ray photoelectron spectroscopy of thin  $\text{Mn}_x\text{Co}_{3-x}\text{O}_4$  ( $1 \geq x \geq 0$ ) spinel films prepared by low-temperature spray pyrolysis. *Thin Solid Films* **311**, 51–57 (1997)
- Guo, J., Lua, A.C.: Microporous activated carbons prepared from palm shell by thermal activation and their application to sulfur dioxide adsorption. *J. Colloid Interface Sci.* **251**, 242–247 (2002)
- Guo, J.X., Liang, J., Chu, Y.H., Sun, M.C., Yin, H.Q., Li, J.J.: Desulfurization activity of nickel supported on acid-treated activated carbons. *Appl. Catal. A* **421**, 142–147 (2012)
- Guo, X.G., Mao, D.S., Lua, G.Z., Wang, S., Wu, G.S.: The influence of La doping on the catalytic behavior of Cu/ZrO<sub>2</sub> for methanol synthesis from  $\text{CO}_2$  hydrogenation. *J. Mol. Catal. A* **345**, 60–68 (2011)
- Guo, X.Y., Bartholomew, C., Hecker, W., Baxter, L.L.: Effects of sulfate species on  $\text{V}_2\text{O}_5/\text{TiO}_2$  SCR catalysts in coal and biomass-fired systems. *Appl. Catal. B* **92**, 30–40 (2009)
- Hammond, J.S., Winograd, N.: XPS spectroscopic study of potentiostatic and galvanostatic oxidation of Pt electrodes in  $\text{H}_2\text{SO}_4$  and  $\text{HClO}_4$ . *J. Electroanal. Chem.* **78**, 55–69 (1977)
- Hudak, S.J., Boerio, F.J., Clark, P.J., Okamoto, Y.: XPS analysis of the interphase between an anaerobic adhesive and metal substrates. *Surf. Interface Anal.* **15**, 167–172 (1990)
- Kazempour, M., Ansari, M., Tajrobehkar, S., Majdzadeh, M., Kermani, H.R.: Removal of lead, cadmium, zinc, and copper from industrial wastewater by carbon developed from walnut, hazelnut, almond, pistachio shell, and apricot stone. *J. Hazard. Mater.* **150**, 322–327 (2008)
- Kobayashi, Y., Ishida, S., Ihara, K., Ihara, K., Yasuda, Y., Morita, T., Yamada, S.: Synthesis of metallic copper nanoparticles coated with polypyrrole. *Colloid Polym. Sci.* **287**, 877–880 (2009)
- Kónya, Z., Vesselenyi, I., Kiss, J., Farkas, A., Oszkó, A., Kiricsi, I.: XPS study of multiwall carbon nanotube synthesis on Ni-, V-, and Ni, V-ZSM-5 catalysts. *Appl. Catal. A* **260**, 55–61 (2004)
- Lee, Y.W., Park, J.W., Choung, J.H., Choi, D.K.: Adsorption characteristics of  $\text{SO}_2$  on activated carbon prepared from coconut shell with potassium hydroxide activation. *Environ. Sci. Technol.* **36**, 1086–1092 (2002)
- Li, H., Jin, Z., Song, H.Y., Liao, S.J.: Synthesis of Co submicro-spheres self-assembled by Co nanosheets via a complexant-assisted hydrothermal approach. *J. Magn. Magn. Mater.* **322**, 30–35 (2010)
- Li, J.J., Kobayashi, N., Hu, Y.Q.: Performance of  $\text{V}_2\text{O}_5/\text{AC}$  activated with the flue gas on  $\text{SO}_2$  removal. *J. Environ. Eng.* **4**, 176–187 (2009)
- Li, K.X., Ling, L.C., Lu, C.X., Liu, Z.Y., Liu, L., Mochida, I.: Influence of CO-evolving groups on the activity of activated carbon fiber for  $\text{SO}_2$  removal. *Fuel Process. Technol.* **70**, 151–158 (2001)
- Mutel, B., Taleb, A.B., Dessaux, O., Goudmand, P., Gengembre, L., Grimblot, J.: Characterization of mixed zinc-oxidized zinc thin films deposited by a cold remote nitrogen plasma. *Thin Solid Films* **266**, 119–128 (1995)
- Namasivayam, C., Kavitha, D.: IR, XRD and SEM studies on the mechanism of adsorption of dyes and phenols by coir pith carbon from aqueous phase. *Microchem. J.* **82**, 43–48 (2006)
- Nguyen-Thanh, D., Bandoz, T.J.: Effect of transition-metal cations on the adsorption of  $\text{H}_2\text{S}$  in modified pillared clays. *J. Phys. Chem. B* **107**, 5812–5817 (2003)
- Paparazzo, E.: XPS analysis of iron aluminum oxide systems. *Appl. Surf. Sci.* **25**, 1–12 (1986)
- Przepiórski, J.: Deposition of additives onto surface of carbon materials by blending method—general conception. *Mater. Chem. Phys.* **2005**, 1–4 (2005)

- Przepiórski, J., Yoshida, S., Oya, A.: Structure of  $K_2CO_3$ -loaded activated carbon fiber and its deodorization ability against  $H_2S$  gas. *Carbon* **37**, 1881–1890 (1999)
- Qin, Y.J., Chen, J.X., Zhang, J.Y.: Effects of  $CeO_2$  and  $CaO$  composite promoters on the properties of eggshell  $Ni/MgO-Al_2O_3$  catalysts for partial oxidation of methane to syngas. *React. Kinet. Catal. Lett.* **94**, 351–357 (2008)
- Rao, C.N.R., Sarma, D.D., Vasudevan, S., Hegde, M.S.: Study of transition metal oxides by photoelectron spectroscopy. *Proc. R. Soc. London Ser. A* **367**, 239–252 (1979)
- Rochester, C.H., Topham, S.A.: Infrared study of surface hydroxyl groups on haematite. *J. Chem. Soc. Faraday Trans.* **75**, 1073–1088 (1979)
- Roh, H.S., Jun, K.W., Dong, W.S., Park, S.E., Baek, Y.S.: Highly stable Ni catalyst supported on  $Ce-ZrO_2$  for oxy-steam reforming of methane. *Catal. Lett.* **74**, 31–36 (2001)
- Sabio, E., Gonzalez, E., Gonzalez, J.F., Gonzalez-Garcia, C.M., Ramiro, A., Ganan, J.: Thermal regeneration of activated carbon saturated with p-nitrophenol. *Carbon* **42**, 2285–2293 (2004)
- Sinapi, F., Delhalle, J., Mekhalif, Z.: XPS and electrochemical evaluation of two-dimensional organic films obtained by chemical modification of self-assembled monolayers of (3-mercaptopropyl) trimethoxysilane on copper surfaces. *Mater. Sci. Eng. C* **22**, 345–353 (2002)
- Tseng, H.H., Wey, M.Y., Fu, C.H.: Carbon materials as catalyst supports for  $SO_2$  oxidation: catalytic activity of  $CuO-AC$ . *Carbon* **41**, 139–149 (2003)
- Wang, X.Q., Ozkan, U.S.: Characterization of active sites over reduced  $Ni-Mo/Al_2O_3$  catalysts for hydrogenation of linear aldehydes. *J. Phys. Chem. B* **109**, 1882–1890 (2005)
- Wang, X.X.: Low temperature oxidation of TiNi shape memory alloy and its effect on Ni ion release in saline solution. *J. Mater. Sci. Lett.* **17**, 375–376 (1998)
- Wu, J.B., Li, Z.G., Lin, Y.: Porous  $NiO/Ag$  composite film for electrochemical capacitor application. *Electrochim. Acta* **56**, 2116–2121 (2011)
- Yang, J., Qiu, K.Q.: Preparation of activated carbons from walnut shells via vacuum chemical activation and their application for methylene blue removal. *Chem. Eng. J.* **165**, 209–217 (2010)
- Zabihi, M., Haghighi Asl, A., Ahmadpour, A.: Studies on adsorption of mercury from aqueous solution on activated carbons prepared from walnut shell. *J. Hazard. Mater.* **174**, 251–256 (2010)